



Effect of noise on the collective dynamics of a heterogeneous population of active rotators

Cite as: Chaos 31, 043101 (2021); <https://doi.org/10.1063/5.0030266>

Submitted: 21 September 2020 . Accepted: 22 March 2021 . Published Online: 01 April 2021

 V. V. Klinshov, D. A. Zlobin, B. S. Maryshev, and  D. S. Goldobin



View Online



Export Citation



CrossMark

ARTICLES YOU MAY BE INTERESTED IN

[Visibility-graphlet approach to the output series of a Hodgkin–Huxley neuron](#)

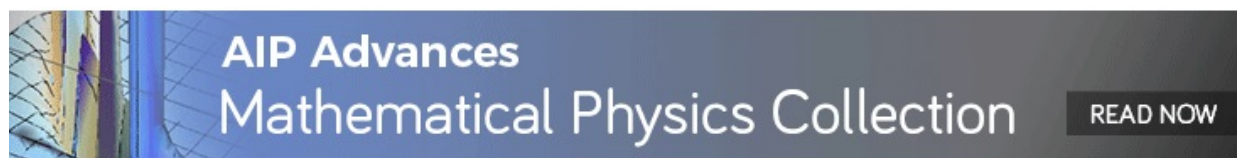
Chaos: An Interdisciplinary Journal of Nonlinear Science **31**, 043102 (2021); <https://doi.org/10.1063/5.0018359>

[Scientometric analysis of the Chaos journal \(1991–2019\): From descriptive statistics to complex networks viewpoints](#)

Chaos: An Interdisciplinary Journal of Nonlinear Science **31**, 043105 (2021); <https://doi.org/10.1063/5.0044719>

[On infinite homoclinic orbits induced by unstable periodic orbits in the Lorenz system](#)

Chaos: An Interdisciplinary Journal of Nonlinear Science **31**, 043106 (2021); <https://doi.org/10.1063/5.0044161>



Effect of noise on the collective dynamics of a heterogeneous population of active rotators

Cite as: Chaos 31, 043101 (2021); doi: 10.1063/5.0030266

Submitted: 21 September 2020 · Accepted: 22 March 2021 ·

Published Online: 1 April 2021




View Online



Export Citation



CrossMark

V. V. Klinshov,^{1,a)}  D. A. Zlobin,¹ B. S. Maryshev,^{2,3,b)} and D. S. Goldobin^{2,3,c)} 

AFFILIATIONS

¹Institute of Applied Physics of the Russian Academy of Sciences, Ulyanova Street 46, 603950 Nizhny Novgorod, Russia

²Institute of Continuous Media Mechanics, UB RAS, Academician Korolev Street 1, 614013 Perm, Russia

³Department of Theoretical Physics, Perm State University, Bukirev Street 15, 614990 Perm, Russia

^{a)}Author to whom correspondence should be addressed: vladimir.klinshov@gmail.com

^{b)}Electronic mail: bmaryshev@mail.ru

^{c)}Electronic mail: Denis.Goldobin@gmail.com

ABSTRACT

We study the collective dynamics of a heterogeneous population of globally coupled active rotators subject to intrinsic noise. The theory is constructed on the basis of the circular cumulant approach, which yields a low-dimensional model reduction for the macroscopic collective dynamics in the thermodynamic limit of an infinitely large population. With numerical simulation, we confirm a decent accuracy of the model reduction for a moderate noise strength; in particular, it correctly predicts the location of the bistability domains in the parameter space.

Published under license by AIP Publishing. <https://doi.org/10.1063/5.0030266>

Large populations of oscillatory or excitable elements are often observed to demonstrate surprisingly low-dimensional and relatively simple collective behavior. The first important breakthrough in the theoretical explanation of the abundance of this “simplicity” was related to the Watanabe–Strogatz and Ott–Antonsen (OA) theories, which were constructed for an important class of popular but idealistic systems. In particular, the latter theory yields an exact self-contained equation for the dynamics of the Kuramoto order parameter. However, the generalization of the OA theory to nonideal phase systems has remained a resisting problem for a decade. An advance with this problem became possible in terms of special order parameters, so-called “circular cumulants,” which are the analog of conventional cumulants but for variables on the circumference. Like conventional cumulants, these variables are a convenient and powerful tool for theoretical studies on many problems, but the convergence of circular cumulant expansions in the general case remains an open question. This issue may become especially delicate when one deals with heterogeneous populations. In such populations, some elements may be close to the bifurcation transitions, where the solutions of the linearized problem possess singularities, which also results in the formal divergence of finite-cumulant approximations. The population of coupled active rotators with

uniform distribution of natural frequencies is an example of such a kind. We construct the theory for this problem and demonstrate that one can handle a singular behavior within the framework of two-cumulant reduction.

I. INTRODUCTION

Collective dynamics of populations of interacting active elements is a subject of continuous researchers’ interest in diverse areas of physics.^{1,2} For a qualitative understanding and description of the collective behavior of such populations, simplistic paradigmatic models are frequently employed. An important class of these models is based on the phase description of the dynamics of individual elements. The assumption of a global character of the interaction between the elements, where all elements are identically mutually coupled to each other, is also abundant in the literature and frequently relevant for populations with a dense network of connections in the thermodynamic limit.^{3,4} For instance, the classic Kuramoto model, which is characterized by the above-mentioned assumptions, allows one to study and describe theoretically the synchronization transition and collective oscillations in great detail.^{5–7}

A recent work⁸ addressed a population of globally coupled active rotators,^{9–11} where some elements oscillate, while the rest of them are in an excitable state. The diversity of the elements of this population results in the formation of a complex structure of domains of different macroscopic regimes in the parameter space; there are time-independent states, mean-field oscillations, and hysteretic transitions between them. The action of intrinsic (in other words, “individual”) noise on the elements of this population does not change the picture qualitatively but significantly shifts the domain boundaries of different regimes.

The influence of the intrinsic noise on the ensemble of active rotators has been studied earlier in a number of papers. First, Shinomoto *et al.*^{9,12} identified the key collective regimes of the system, namely, the stationary and the oscillatory ones, and constructed the bifurcation diagrams numerically. Later, Park and Kim discovered the emergence of clustered states in the case of strong multiplicative noise.¹³ Zaks *et al.* obtained a simple two-dimensional system describing the dynamics of the population in the Gaussian approximation.¹⁴ The next step was made by Tessone *et al.*,¹⁵ who introduced the heterogeneity in the form of inequality of the elements intrinsic parameters. They formulated a simple rule for the qualitative role of the noise: it makes an impact in the same direction as the increase of the diversity of the elements.

Although ensembles of active rotators with intrinsic noise have been studied in a number of papers, a comprehensive quantitative description is still lacking. The theoretical studies carried out in the earlier works address only limited cases, such as high-frequency limit,¹⁶ identical elements,¹⁴ or strong synchronization.¹⁵ The present paper aims to fill the gap and develop a solid theory describing quantitatively the effect of noise on the collective dynamics of a population of coupled active rotators. Our approach is based on the method of circular cumulants, recently developed in a series of works^{17–21} and applicable to a wide class of stochastic oscillatory systems. In the thermodynamic limit of an infinitely large population, we obtain theoretical expressions for stationary states. A bifurcation analysis of the system is also carried out, and the obtained bifurcation curves were shown to describe quite accurately the transitions between different collective modes for a large but finite number of elements in the population.

In systems admitting Ott–Antonsen ansatz, the imperfectness of synchrony in stable regimes is often associated with the heterogeneity of parameters (natural frequencies, etc.). In the case of Lorentzian or some other fractional rational distribution of parameters, one can either (i) first employ the OA ansatz for subpopulations with the same values of parameters and then perform a contour integration over distributed parameters by means of the residue theorem or do these operations in the opposite order; (ii) first perform the contour integration for an infinite chain of the Kuramoto–Daido order parameters and second employ the OA ansatz, which makes all these equations identical to the first equation, leaving one closed equation. If the conditions for the OA ansatz are violated, one can still deal with the infinite chain of equations derived on route (ii) for the order parameters; the series of these parameters decays with the order number in the case of imperfect synchrony (e.g., see Ref. 22). Route (i) becomes impractical as the attracting states of some subpopulations for vanishing violation of the OA conditions are perfect synchrony ones and one has to work in the vicinity of a

state, where the infinite equation chain does not converge. When one deals with such parameter heterogeneity, the infinite chains of equations for Kuramoto–Daido order parameters of subpopulations often become an inapplicable framework. Meanwhile, the alternative circular cumulant framework can not only be just possible but also convenient. The case of coupled noisy active rotators with non-fractional–rational distribution of frequencies is an example of such sort; part of subpopulations in this system is always perfectly synchronized in the absence of noise.

Although a large part of our study is applicable to ensembles with an arbitrary distribution of intrinsic parameters, the bifurcation curves are plotted for a particular case of uniform distribution. Considering the effect of noise on the collective dynamics of such a population, one should bear in mind the remarkable degeneracy of the Kuramoto system with a uniform distribution of natural frequencies, as adopted in Ref. 8. Generally speaking, this degeneracy takes place for any distribution, which has a plateau in its structure.^{23–25} For vanishing noise, at the threshold of the collective mode emergence, there is not a single attracting state, but a one-parameter family of states. In this case, the transition to synchronization is a first-order phase transition: the order parameter has a finite value immediately above the threshold. But this is not the ordinary case of a subcritical pitchfork bifurcation; below the threshold, the maximal asynchrony regime is the only stable one. Weak noise eliminates this degeneracy, and the transition to synchronization becomes a transition of the second order [for example, see the dependence of Eq. (131) in Ref. 6 vs the intensity of the intrinsic noise D]. The system of active rotators, however, differs from the classic Kuramoto ensemble since the nonuniform phase rotation breaks the degeneracy even for a vanishing noise. Nevertheless, the described feature of the Kuramoto system indicates the necessity for a thorough analysis of the effect of noise in the case of active rotators as well.

This paper is organized as follows. In Sec. II, the model under study is introduced. In Sec. III, the elements of the circular cumulant approach relevant to our problem are briefly provided. In Sec. IV, we employ the circular cumulant approach to construct the mean-field theory for the population of noisy active rotators with uniform distribution of frequencies. The results of the bifurcation analysis on the basis of the theory constructed are provided in Sec. V. Conclusions are drawn in Sec. VI.

II. MODEL

We consider a heterogeneous population of N coupled active rotators governed by the Langevin equations,⁸

$$\dot{\theta}_j = \omega_j - a \sin \theta_j - \frac{K}{N} \sum_k \sin(\theta_j - \theta_k + \alpha) + \sigma \eta_j(t). \quad (1)$$

Here, the elements are indexed with $j = 1, 2, \dots, N$, $\theta_j \in S^1$ are the phases of elements, the rotation nonuniformity parameter a is assumed to be identical for all elements, and ω_j is an intrinsic parameter, which is frequently referred to as “natural frequency.” Notice that it is not an actual frequency, as the natural oscillation period of

a single rotator nonlinearly depends on the parameter ω ,

$$T = \frac{2\pi}{\sqrt{\omega_j^2 - a^2}}.$$

One can see that $T = 2\pi/|\omega_j|$ only for $|\omega_j| \gg a$. Moreover, for $|\omega_j| < a$, an uncoupled element does not oscillate but rests in an locally stable equilibrium state $\theta = \arcsin(\omega_j/a)$. Thus, the parameter ω_j governs the inherent dynamics of the j th element, which is excitable for $|\omega_j| < a$ and oscillating for $|\omega_j| > a$.

The interaction between elements is described by the sum in the right-hand side of Eq. (1), where the coupling is assumed to be global and characterized by the strength K and the phase shift α . Each element is subject to intrinsic (individual) fluctuations, which are represented by white Gaussian noise signals $\sigma\eta_j(t)$ of intensity $2\sigma^2$; the fluctuations for different elements are independent: $\langle \eta_j(t) \rangle = 0$, $\langle \eta_j(t)\eta_k(t') \rangle = 2\delta_{jk}\delta(t-t')$.

Equation system (1) can be recast as

$$\dot{\theta}_j = \omega_j + \text{Im}(2he^{-i\theta_j}) + \sigma\eta_j(t), \quad (2)$$

where $2h = a + KRe^{-i\alpha}$, and

$$R = \langle e^{i\theta_j} \rangle = \frac{1}{N} \sum_j e^{i\theta_j}$$

is the complex-valued Kuramoto order parameter. In the recent series of works,^{17,18,20} a systematic approach to studying the systems of type (2) was suggested on the basis of so-called ‘‘circular cumulants.’’ Below, we briefly recall the principal details of this approach and derive the equations relevant for our study.

III. CIRCULAR CUMULANT APPROACH

In the thermodynamic limit $N \rightarrow \infty$, the state of system (1) can be comprehensively characterized by the probability density function $\rho(\theta|\omega, t)$ obeying the normalization condition $\int_0^{2\pi} \rho(\theta|\omega, t)d\theta = 1$ and governed by the corresponding Fokker-Planck equation [cf. Eq. (9) in Ref. 9],

$$\frac{\partial \rho}{\partial t} = -\frac{\partial}{\partial \theta} (\rho [\omega + \text{Im}(2h(t)e^{-i\theta})]) + \sigma^2 \frac{\partial^2 \rho}{\partial \theta^2}. \quad (3)$$

The probability density can be recast in the form of the Fourier series

$$\rho(\theta|\omega, t) = \frac{1}{2\pi} \sum_n z_n(\omega, t)e^{-in\theta},$$

where coefficients

$$z_n(\omega, t) = \int_0^{2\pi} \rho(\theta|\omega, t)e^{in\theta} d\theta \quad (4)$$

are the ‘‘local’’ order parameters characterizing the distribution of phases of the elements with ‘‘frequency’’ ω . Below, we do not indicate the dependence of z_n on ω but imply it. The order parameters obey the equation system,

$$\dot{z}_n = ni\omega z_n + nhz_{n-1} - nh^*z_{n+1} - n^2\sigma^2 z_n, \quad (5)$$

where an asterisk stands for complex conjugation. Notice that for vanishing noise ($\sigma = 0$), system (5) admits the Ott–Antonsen ansatz

$z_n = (z_1)^n$ (see Refs. 26 and 27), which yields a single equation

$$\dot{z} = i\omega z + h - h^*z^2.$$

Here, index ‘‘1’’ is omitted. However, even for a weak noise, the Ott–Antonsen ansatz becomes inadmissible, and Eq. (5) forms an infinite chain. The same infinite chain of equations was obtained in Refs. 9 and 14. In the case of imperfect synchrony, the series of the order parameters $|z_n|$ decays with the order number.²² However, the decay rate might be quite slow: for example, Shinomoto and Kuramoto had to retain the first 30–50 order parameters in order to construct the bifurcation diagrams.⁹ An alternative approach is to assume Gaussian distribution of phases, as was done by Zaks *et al.*¹⁴ This allows one to express the order parameters via the mean and the variance, but the Gaussian approximation is limited to the case of high synchrony. In the heterogeneous ensemble, the synchronization degree may be different for subpopulations with different ω , which requires a universal approach applicable for both strongly and weakly synchronous cases. It turns out that the representation of Eq. (5) in terms of the so-called ‘‘circular cumulants’’ provides such an approach; this approach turns out to be much more handy.

There is an essential geometric difference between random variables on the circumference and on the infinite real line. Because of this difference, the modification of conventional cumulants,^{28,29} which were introduced for the variables on the line, is required in some physical problems. For the definition of the circular cumulants, let us introduce the moment-generating function

$$F(k, t) = \langle \exp(ke^{i\theta}) \rangle = \sum_{m=0}^{\infty} z_m \frac{k^m}{m!},$$

where $z_m = \frac{\partial^m}{\partial k^m} F(k, t)|_{k=0}$. Taking the time derivative of this function and substituting \dot{z}_m from (5), one can obtain

$$\frac{\partial F}{\partial t} = i\omega k \frac{\partial F}{\partial k} + hkF - h^*k \frac{\partial^2}{\partial k^2} F - \sigma^2 k \frac{\partial}{\partial k} \left(k \frac{\partial F}{\partial k} \right). \quad (6)$$

Further, we define the circular cumulants as the coefficients of the Taylor series of the generating function

$$\Psi(k, t) = k \frac{\partial}{\partial k} \ln(F(k, t)) = \sum_{m=1}^{\infty} \varkappa_m(t) k^m,$$

where $\varkappa_m = \frac{1}{m!} \frac{\partial^m}{\partial k^m} \Psi(k, t)|_{k=0}$. Circular cumulants are unambiguously determined by the order parameters z_m ; for instance, the first three cumulants are

$$\varkappa_1 = z_1, \quad \varkappa_2 = z_2 - z_1^2, \quad \varkappa_3 = (z_3 - 3z_2z_1 + 2z_1^3)/2.$$

From (6), one finds that the cumulant-generating function obeys the following partial derivative equation:

$$\begin{aligned} \frac{\partial \Psi}{\partial t} = & i\omega k \frac{\partial \Psi}{\partial k} + hk - h^*k \frac{\partial}{\partial k} \left(k \frac{\partial}{\partial k} \left(\frac{\Psi}{k} \right) + \frac{\Psi^2}{k} \right) \\ & - \sigma^2 k \frac{\partial}{\partial k} \left(k \frac{\partial \Psi}{\partial k} + \Psi^2 \right). \end{aligned}$$

This equation yields an infinite chain of equations for the circular cumulants,

$$\dot{\varkappa}_n = ni\omega\varkappa_n + h\delta_{1n} - h^* \left(n^2\varkappa_{n+1} + n \sum_{m=1}^n \varkappa_{n+1-m}\varkappa_m \right) - \sigma^2 \left(n^2\varkappa_n + n \sum_{m=1}^{n-1} \varkappa_{n-m}\varkappa_m \right). \tag{7}$$

At the first glance, these equations look more cumbersome than (5). However, an important advantage of the series (7) is that for a weak noise $\sigma \ll 1$, the cumulants form a smallness hierarchy $\varkappa_n \sim \sigma^{2(n-1)}$. The presence of this hierarchy follows from the form of Eq. (7) and does not depend on the synchronization degree. It will be further confirmed by the numerical simulations. This allows one to restrict the consideration to the first M cumulants and set the higher cumulants to zero, which yields an approximation with an inaccuracy of the order of magnitude of σ^{2M} . In what follows, we employ the two-cumulant approximation assuming $\varkappa_3 = \varkappa_4 = \dots = 0$. Note that other approximations for the higher cumulants are possible (see Ref. 18 for details). However, we found out that these approximations do not lead to the accuracy improvement for our system; therefore, we chose to use the simplest one. Hence, for the dynamics of the first two cumulants of the subpopulation with natural frequency ω , we find the following equation system:

$$\dot{z}(\omega, t) = i\omega z + h - h^*(z^2 + \varkappa) - \sigma^2 z, \tag{8}$$

$$\dot{\varkappa}(\omega, t) = 2i\omega\varkappa - 4h^*z\varkappa - \sigma^2(4\varkappa + 2z^2), \tag{9}$$

where $z(\omega, t)$ is the first cumulant (identical to the local Kuramoto order parameter) and $\varkappa(\omega, t)$ is the second one. Thus, the dynamics of the subpopulation at given ω can be (approximately) described by just two equations for the first two cumulants instead of an infinite series (5) for the order parameters. Once the first two cumulants are known (and the higher ones are assumed to be zero), the order parameters z_n can be readily calculated as $z_n = z^n + \frac{n(n-1)}{2}\varkappa z^{n-2}$.

Let us elucidate the geometric interpretation of the two-cumulant representation. For the conventional cumulants of variables on the real line, there is a special case of the Gaussian distribution, which possesses exactly two nonzero cumulants. The first conventional cumulant is the mean value, giving the centering of the distribution, and the second conventional cumulant is the variance, measuring the distribution width. If any other conventional cumulant is nonzero, there are infinitely many nonzero elements.^{28,30} For variables of the circumference, the special case is the Ott–Antonsen case with the wrapped Lorentzian distribution; here, only the first circular cumulant $z = \varkappa_1$ is nonzero, but this number is complex-valued. Its argument gives the distribution centering, and its absolute value characterizes the distribution width, $-\ln|\varkappa_1|$. If more than one circular cumulant is nonzero, there are infinitely many nonzero elements.²⁰ Thus, the Ott–Antonsen case is the only case with a finite number of nonzero circular cumulants. Comparing these two cases of distributions on the line and on the circumference, one can speak of equity, as the minimalistic picture comes with two nontrivial quantities in both cases.

Further, if one considers the deviation from the Gaussian distribution, it is primarily quantified by two numbers: the third

conventional cumulant, or *skewness*, characterizing the distribution asymmetry and the fourth conventional cumulant, proportional to *kurtosis*, characterizing the excess of tails. For variables on the circumference, the complex-valued second circular cumulant yields two quantifiers: the argument difference $\text{Arg}\varkappa_2 - 2\text{Arg}\varkappa_1$ measures the distribution asymmetry and $|\varkappa_2|$ characterizes the tails.

The theoretical analysis below is based on equation system (8) and (9), which generally possesses the inaccuracy of the order of magnitude of σ^4 . Importantly, if the dependence of the local order parameters $z(\omega)$ on the element parameter ω possesses singularities or derivative discontinuities, then the order of inaccuracy of finite cumulant truncations is not guaranteed. Below, we will see that such a discontinuity is present in the problem we consider.

IV. ANALYSIS WITHIN THE FRAMEWORK OF THE CIRCULAR CUMULANT DESCRIPTION

The coupling in population (1) is global; therefore, subpopulations (8) and (9) with different ω are coupled via a common mean field. In the thermodynamic limit, this mean field is given by the integral

$$R(t) = \langle e^{i\theta} \rangle = \int d\omega g(\omega) z(\omega, t), \tag{10}$$

where $g(\omega)$ is the natural frequency distribution. Let us consider the case where the mean field is time-independent. In this case, it is convenient to write

$$h = \frac{1}{2}Be^{i\beta}$$

and make the change of variables $\xi(\omega) = z(\omega)e^{-i\beta}$. Then, the time-independent states of (8) and (9) are given by the solutions of

$$B\xi^2 - 2i\omega\xi - B = -\sigma^2\xi \left(2 + \frac{B\xi}{i\omega - B\xi - 2\sigma^2} \right). \tag{11}$$

For $\sigma = 0$, the solutions of (11) satisfying $|\xi| \leq 1$ have the form

$$\xi_0(\omega) = \begin{cases} \sqrt{1 - \frac{\omega^2}{B^2}} + i\frac{\omega}{B}, & |\omega| < B, \\ i\frac{\omega}{B} \left(1 - \sqrt{1 - \frac{B^2}{\omega^2}} \right), & |\omega| > B. \end{cases} \tag{12}$$

One can see that $|\xi_0| = 1$ for $|\omega| < B$, and $|\xi_0| < 1$ for $|\omega| > B$. This property elucidates the physical significance of B : in the noise-free case, the elements with a small natural frequency $|\omega| < B$ are entrained by the mean field and rest, while the element with higher $|\omega| > B$ rotate.

For a weak noise, we seek for the solutions of (11) in a perturbative form, $\xi(\omega) = \xi_0(\omega) + \nu(\omega)$. Keeping only linear in ν and σ^2 terms, after some algebra, we arrive at

$$\nu(\omega) = \frac{B\sigma^2}{2(\omega^2 - B^2)}. \tag{13}$$

Expression (13) diverges for $|\omega| = B$, which is the result of the linearization of a square-root dependence of $\xi_0(\omega)$ near $|\omega| = B$ in Eq. (12). This is the above-mentioned case of the decrease of the

accuracy order due to derivative discontinuities; linear approximation is not appropriate here and we will consider this case separately. Taking into account that $\xi_0(\pm B) = \pm i$ and keeping only the leading in ν and σ terms, from (11), we obtain

$$[\nu(\pm B)]^3 = -\frac{\sigma^2}{B}. \tag{14}$$

Since z is the Kuramoto order parameter, its absolute value cannot exceed one. The only solution satisfying $|\xi_0 + \nu| \leq 1$ is

$$\nu(\pm B) = \sqrt[3]{\frac{\sigma^2}{B} \frac{1 \mp i\sqrt{3}}{2}}. \tag{15}$$

For the regularization of the noise-induced shifts (13) near the singular points, let us construct an expression, which is close to (15) at the points $\omega = \pm B$, and close to (13) far from these points. The simplest way to construct such an expression is to add a small complex number to the denominator of (13). While a real-valued addition just shifts the singularity point along ω , a nonzero imaginary part of the addition shifts the singularity away from the real line of ω . We choose the value of this addition, which provides a required value of $\nu(\pm B)$, and arrive at

$$\nu(\omega) = \frac{B\sigma^2}{2(\omega - B + \epsilon)(\omega + B - \epsilon^*)}, \tag{16}$$

where

$$\epsilon = \sigma \sqrt[3]{B\sigma} \frac{1 + i\sqrt{3}}{8}. \tag{17}$$

Equation (16) approximates the noise-induced shift of the order parameter z of the subpopulation with frequency ω . To estimate the accuracy of this approximation, we compare it with the exact solution of (11). Note also that system (8)–(9) is an approximation itself; therefore, it is also important to perform the comparison to the results obtained for the “exact” numeric solution of the Fokker–Planck equation (3). In Fig. 1, the shift ν of the order parameter z is plotted vs the natural frequency ω for three different ways of calculation: with Eq. (16), with the exact solution of (8) and (9), and with the “exact” solution of the Fokker–Planck Eq. (3). The results are provided for three different values of noise strength σ and fixed $B = 1$. As expected, the noise mostly influences the elements close to the local bifurcation points $\omega = \pm B$. However, with the growth of the noise strength, the peak shifts toward smaller frequencies and becomes broader. Far from the central peak there is a good correspondence between the exact solution and both its approximations, while near the peak the correspondence is only qualitative. However, the two-cumulant approximation can be appropriate as the collective dynamics is controlled by the mean field, which is an integral over ω and the contribution of the error in a narrow vicinity of the bifurcation point might be negligible.

The accuracy of the two-cumulant approximation improves as the noise strength decreases. To determine the accuracy order of the approximation we calculate the error χ for the value of the Kuramoto order parameter. In Fig. 2, the error of expression (16) with respect to the exact solution of the Fokker–Planck equation is plotted vs the noise strength σ for three different frequency values ω . The order of the magnitude of the error strongly depends on the

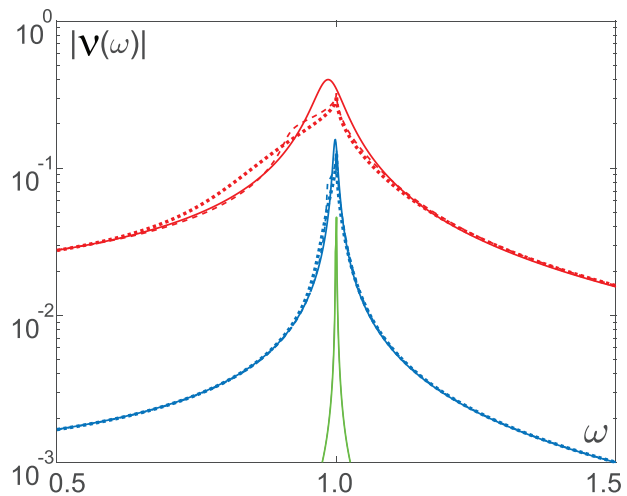


FIG. 1. The noise-induced shift ν of the Kuramoto order parameter z is plotted vs the natural frequency ω for three values of the noise strength; from bottom to top, $\sigma = 0.01$ (green), $\sigma = 0.05$ (blue), and $\sigma = 0.2$ (red). Solid lines: formula (16), dashed lines: exact solution of (11), and bold dotted line: “exact” numeric solution of (3).

proximity of ω to the bifurcation points $\pm B$. Far from the bifurcation point, the error decreases as $\chi \sim \sigma^{10/3}$. Indeed, formula (16) approximates the exact solution of (11) with the inaccuracy of the order of magnitude of $\sigma^2\epsilon \sim \sigma^{10/3}$, while the inaccuracy of the two-cumulant approximation itself is of the order of σ^4 . However, for $\omega = B$, the accuracy is much worse and the error decreases only as $\chi \sim \sigma^{2/3}$. This decrease in accuracy is due to the fact that formula (16) is introduced for the regularization of the formal divergence of the linear approximation (13): it provides only a rough approximation for ν in the neighborhood of $\omega = \pm B$. Indeed, in Fig. 1, one can see that in this neighborhood, the error of determination of $\nu(\omega)$ is commensurable to its value, which is $\sim \sigma^{2/3}$.

Let us now estimate the accuracy of the calculation of the mean field of the whole population using approximation (16). The error of the calculation of integral (10) with formula (16) can be decomposed into two contributions: (i) the contribution of the neighborhood of the singularity points $\omega = \pm B$ and (ii) the contribution of the domains far from these points. The contribution of the singularities cannot exceed $|\epsilon||\nu(B)| \sim \sigma^{4/3}\sigma^{2/3} = \sigma^2$, while the contribution of the domains beyond the singularity vicinities is of the order $\sigma^{10/3}$. Thus, using formula (16), one can calculate the population mean field with the inaccuracy not worse than σ^2 . This order of precision is confirmed by Fig. 2, which shows the mean error for the calculation of the Kuramoto order parameter for the interval $\omega \in [0; 1.5]$ vs the noise strength. As expected, the error decreases as σ^2 .

According to the theoretical results presented here and below, the change in the characteristics of the macroscopic behavior of the system under the influence of noise is $\propto \sigma^2$, which is of the same order of magnitude as the error. Therefore, regularization (16) can be treated as an approximation but not as a rigorous expansion with respect to a small parameter σ^2 . A rigorous expansion

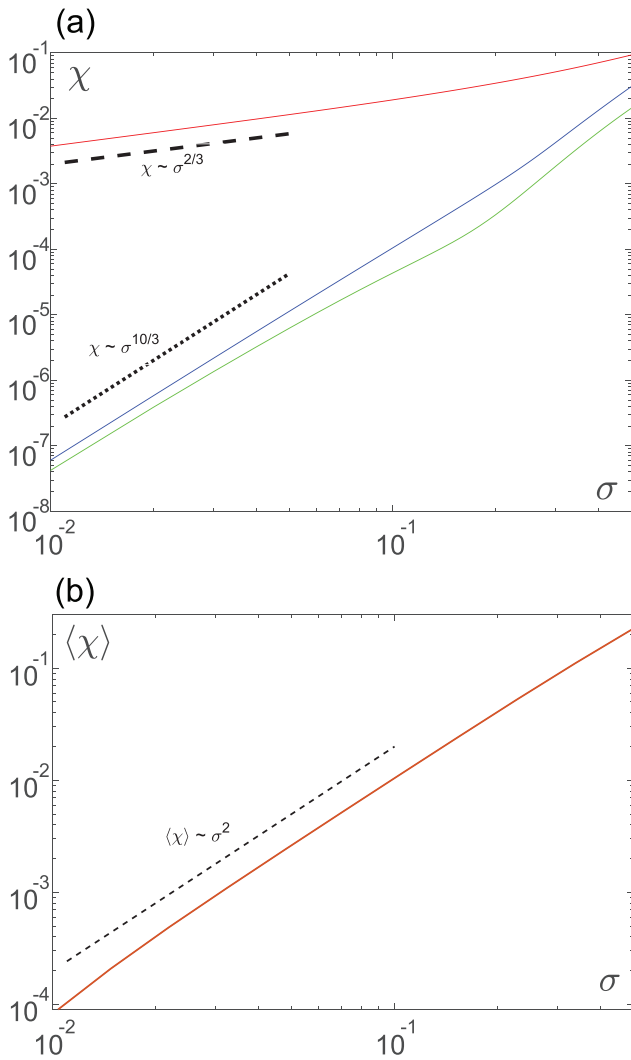


FIG. 2. (a) Error χ of the Kuramoto order parameter calculated with (16) vs the noise strength σ for three different frequencies: from bottom to top, $\omega = 1.5$ (green), $\omega = 0.5$ (blue), and $\omega = 1$ (red). Dashed line: $\chi \propto \sigma^{2/3}$ and dotted line: $\chi \propto \sigma^{10/3}$. (b) The mean value of error $\langle \chi \rangle$ of the calculation of the Kuramoto order parameter on the interval $\omega \in [0; 1.5]$ is plotted vs the noise strength σ . The dashed line indicates the slope $\chi \propto \sigma^2$.

accurately dealing with the singular points of the linearized problem is cumbersome and is not presented in this paper. With the rigorous expansion, the error would also not be $\propto \sigma^4$, as in “convenient” situations,^{17,18} but increased due to the integration over ω of the function diverging at $\omega = \pm B$ for $\sigma = 0$. Nonetheless, the comparison of the theoretical findings to the results of numerical simulation confirms that our approximation is fairly accurate.

Let us now consider the macroscopic dynamics of the whole population. Obviously, the local order parameters of subpopulations depend on the parameter B , which in turn depends on the

global order parameter R . Taking into account that the global order parameter is obtained from the local ones by averaging over the entire population, it is possible to write down the condition for the self-consistency of a stationary state with a time-independent mean field,

$$R = \rho e^{i\psi} = \int d\omega g(\omega) z(\omega).$$

Substituting $z = (\xi_0 + \nu)e^{i\beta}$, one can rewrite this condition as

$$\rho e^{i(\psi-\beta)} = \frac{i}{B} f_1(B) + \frac{1}{B} f_2(B),$$

where

$$f_1(B) = \Omega - \int_{|\omega|>B} d\omega g(\omega) \omega \sqrt{1 - \frac{B^2}{\omega^2}} + B\phi_1, \tag{18}$$

$$f_2(B) = \int_{|\omega|<B} d\omega g(\omega) \sqrt{B^2 - \omega^2} + B\phi_2,$$

$\phi_1(B)$ and $\phi_2(B)$ are the imaginary and real parts of the integral

$$\int d\omega g(\omega) \nu(\omega) = i\phi_1 + \phi_2, \tag{19}$$

$\nu(\omega)$ is given by (16), and $\Omega = \langle \omega \rangle$ is the mean frequency of the population. Finally, after some algebra, this condition can be recast as

$$f(B) = B^2 - a^2 - 2K(f_1(B) \sin \alpha + f_2(B) \cos \alpha) + K^2 \frac{f_1^2(B) + f_2^2(B)}{B^2} = 0. \tag{20}$$

Solutions of (20) yield the values of B , satisfying the self-consistency condition.

Following Ref. 8, we consider a uniform distribution of frequencies,

$$g(\omega) = \begin{cases} 0, & \omega < \omega_1, \\ \gamma, & \omega_1 < \omega < \omega_2, \\ 0, & \omega > \omega_2, \end{cases} \tag{21}$$

where $\gamma = 1/(\omega_2 - \omega_1)$ according to the normalization condition. For this distribution $\Omega = (\omega_1 + \omega_2)/2$, and it is also convenient to introduce the distribution width $\Delta = \omega_2 - \omega_1$. In this case, integral (19) can be evaluated as

$$i\phi_1 + \phi_2 = I(\omega_2) - I(\omega_1), \tag{22}$$

where

$$I(\omega) = \gamma \int_0^\omega \nu(\omega') d\omega' = \frac{\gamma B \sigma^2}{4(B - \text{Re}\epsilon)} \ln \frac{\omega - B + \epsilon}{\omega + B - \epsilon^*}. \tag{23}$$

In Fig. 3, typical shapes of the function $f(B)$ are presented for various values of σ . One can see that noise can change the curve shape significantly and, thus, shift the values of B resolving the self-consistency condition and even change the number of roots. Below, we consider the effect of noise on the collective modes and their bifurcations in detail.

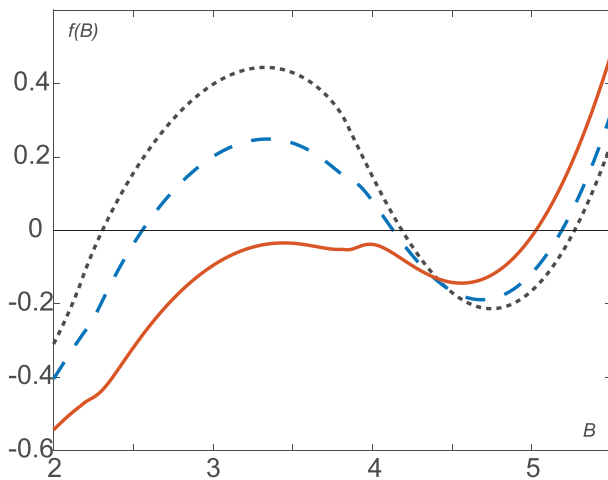


FIG. 3. A typical shape of function $f(B)$ is plotted for various values of the noise strength: $\sigma = 0$ (black dotted line), $\sigma = 0.3$ (blue dashed line), and $\sigma = 0.5$ (red solid line). The other parameters are $\Omega = 0.82$, $\Delta = 6$, $K = 5$, $a = 1$, and $\alpha = 0$.

V. RESULTS

Noise-free system (1) was reported in Ref. 8 to demonstrate various collective modes depending on its parameter values. The principle modes are (i) the rest state where none of the elements oscillate, (ii) the asynchronous oscillatory mode, and (iii) the synchronous oscillatory mode characterized by periodic oscillations of the mean field R . Moreover, bistability domains were found in the parameter space where the system can demonstrate different behavior depending on its initial state. In the presence of noise, the qualitative structure of the parameter space is preserved, but the boundaries of the domains are significantly shifted.

The theory developed above makes it possible not only to explain the observed persistence of low-dimensional collective dynamics under conditions where the Ott–Antonsen theory ceases to be applicable but also to quantitatively describe the effect of noise on the population. To obtain the possible collective regimes for a given set of parameters, one needs to solve Eq. (20) for B , which gives the values of the mean field R of the population. Moreover, it also allows one to describe the microscopic dynamics of the population, i.e., the dynamics of individual oscillators. Given the global order parameter B , the local Kuramoto order parameter $z(\omega)$ can be calculated from (12) and (16). In Fig. 4, the theoretical predictions are compared with the results of direct numerical simulation of an ensemble of $N = 10\,000$ active rotators whose frequencies were uniformly distributed from ω_1 to ω_2 (in other trials the frequencies were randomly drawn from the uniform distribution which led to the same results). For the selected parameter values, Eq. (20) has a unique solution corresponding to a stable time-independent state. The temporal evolution of the mean field plotted in Fig. 4(a) confirms that it quickly converges to the theoretically predicted value. Small fluctuations near the stationary state correspond to the finite-size effects. The microscopic state of the ensemble is heterogeneous

since some units fluctuate below the threshold while others rotate more or less regularly, as can be seen from the phase dynamics presented in Fig. 4(b). The local Kuramoto order parameter $|z(\omega)|$ is close to one for the units fluctuating below the threshold and less than one for the rotating ones, as shown in Fig. 4(c). The theory predicts the local order parameter fairly accurately and, therefore, allows us to discriminate between the fluctuating and rotating units.

The cumulant-based approach allows us to predict the macroscopic dynamics of the population in a broad range of parameter values. In Fig. 4(d), the mean field observed in numerics is compared with the theoretically predicted value. Note that the correspondence between the theoretical and numerical values is good even for a strong noise when the mean field is well below 1, i.e., the ensemble is weakly synchronized.

Furthermore, it is possible to predict not only quantitative but also qualitative changes in the population behavior and determine the boundaries of the domains of different modes of collective dynamics. These boundaries correspond to bifurcations of the system, among which the saddle-node bifurcation plays an important role. In particular, the saddle-node bifurcation corresponds to the transition from the rest state to the synchronous oscillatory mode, as well as the transitions between bistability and monostability domains.

The saddle-node bifurcation corresponds to the tangency of the graph of the function $f(B)$ to the horizontal axis, which allows one to find the bifurcation points. In Fig. 5, the bifurcation curves are plotted on the plane of (Δ, Ω) for several values of the noise strength σ . In the no-noise case ($\sigma = 0$), two lines of the saddle-node bifurcation form a typical “tongue” first reported by Shinomoto and Kuramoto.⁹ The system possesses three equilibrium states inside the tongue, while outside it, only one state is present. Note that the bistability region occupies only a part of the tongue-shaped area near the cusp point, namely, the bistability region is bounded by two lines of the saddle-node bifurcations and a saddle homoclinic bifurcation curve. The detailed description of the bifurcations in the noiseless case is given in Ref. 8.

In the presence of noise, the structure of the bifurcation curves is qualitatively preserved, although they are significantly shifted. Note that for intermediate values of the noise strength, the structure of the saddle-node bifurcation curves becomes somewhat more sophisticated, which is associated with the appearance of a small additional extrema of the function $f(B)$. However, the tongue-shaped region persists on the parameter plane; inside this tongue, the system still has three (or more) equilibrium states and a single equilibrium state outside. With increasing noise intensity, the tongue-shaped domains of multistability shift to lower values of Δ . Previously, this behavior was qualitatively interpreted as an effective increase in the parameter spread due to the action of noise.^{8,15} With the approach developed in this work, one can describe this effect quantitatively. In Fig. 6, the dependence of the bifurcation threshold Δ_{SN} on the noise strength is presented for several values of Ω . One can see a lowering bifurcation threshold with the noise intensity growing.

To confirm the theoretical results obtained with the two-cumulant approach, the bifurcation diagrams were compared to the results of direct numerical simulation of a population of $N = 10\,000$ active rotators. The noise strength was fixed at $\sigma = 0.3$, and the

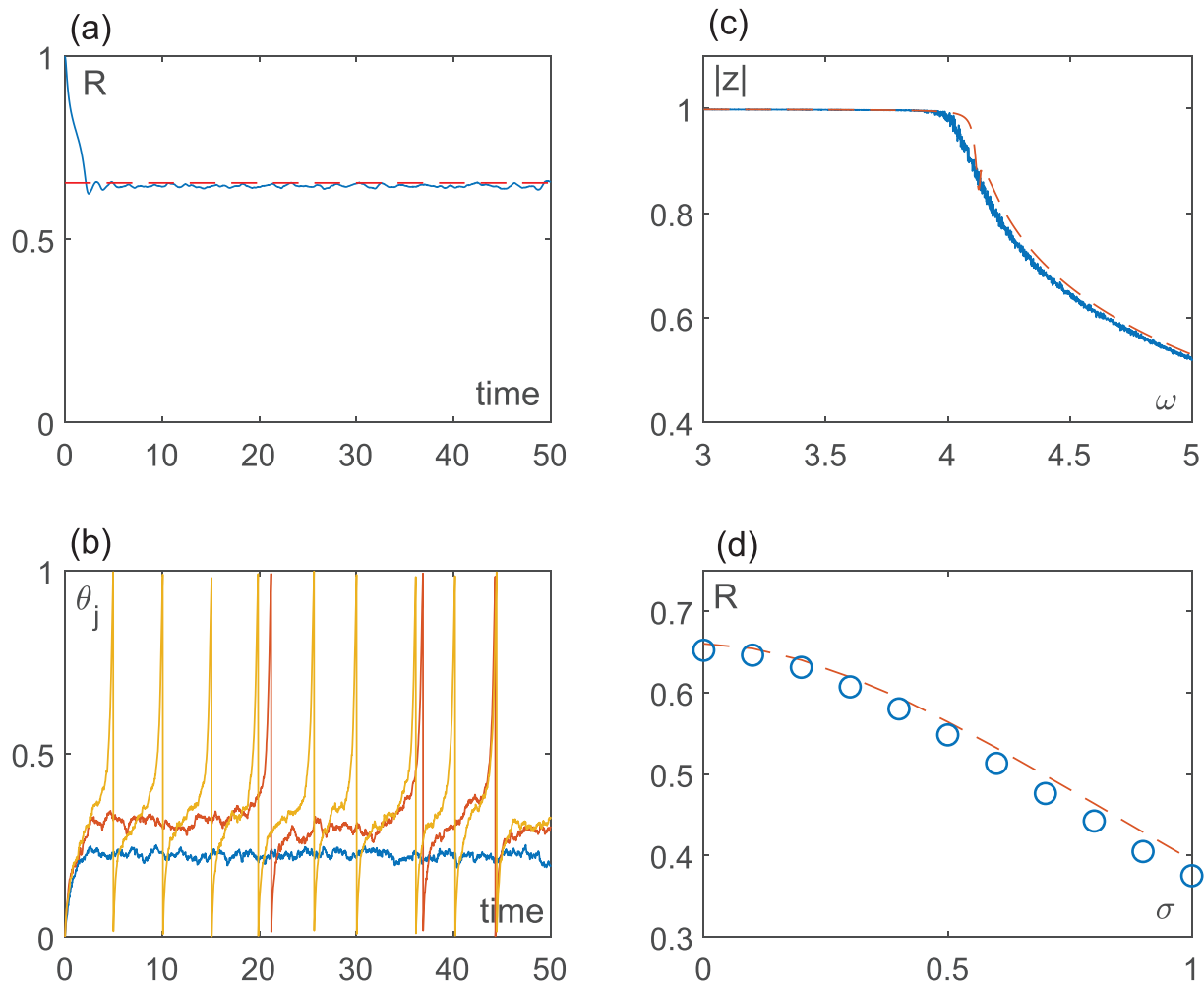


FIG. 4. The dynamics of the ensemble of $N = 10^4$ active rotators is presented for $\Omega = 0.8$, $\Delta = 10$, $K = 5$, $a = 1$, and $\alpha = 0$. (a) The temporal evolution of the mean field (blue solid line) and the theoretically predicted time-independent state (red dashed line) for the noise intensity $\sigma = 0.1$. (b) The phase dynamics of the three units with $\omega = 3.3$ (blue line), $\omega = 4.1$ (red line), and $\omega = 4.3$ (yellow line). (c) The local Kuramoto order parameter $z(\omega)$: numerical results (blue solid line) and theoretical predictions (red dashed line). (d) The mean field R vs the noise strength σ : numerical results (blue circles) and theoretical predictions (red dashed line).

parameters Ω and Δ were varied over a wide range. For each parameter value, system (1) was integrated several times for the time interval $t = 1000$ with different randomly set initial states. After the initial transient period of $t = 200$, the time-averaged Kuramoto order parameter $\rho = \langle |R| \rangle$ was calculated. As a result, a set of possible collective modes was determined for each set of parameters, and the regions of monostability and bistability were identified. In addition to that, the order parameter $\zeta = \langle |R - \langle R \rangle| \rangle$ was calculated in order to distinguish between the steady states and oscillatory regimes. The diagram of macroscopic regimes is presented in Fig. 7 as a raster plot with the theoretical saddle-node bifurcation curves superimposed. The theoretical and the numerical results are in good agreement: the bistability area is located inside the tongue-shaped region in the vicinity of the cusp point, while the transition to the collective

oscillations takes place on the upper bifurcation curve. Here, the saddle-node bifurcation occurs on a closed contour formed by the unstable manifolds of the saddle; after the disappearance of fixed points, the motion on the contour becomes unidirectional and the contour turns into a limit cycle. This is the conventional “SNIPER” bifurcation.

Note, however, that there are some differences between the theoretical and numerical results. In numerical simulations for a finite population, we were unable to observe any qualitative changes in the dynamics of the system on the “internal” lines of saddle-node bifurcations associated with the small additional extrema of the function $f(B)$ (see the solid line in Fig. 3). Possible reasons include, first, the inaccuracy of the two-cumulant approximation, and, second, finite-size effects, which are inevitable in the numerical study. In a

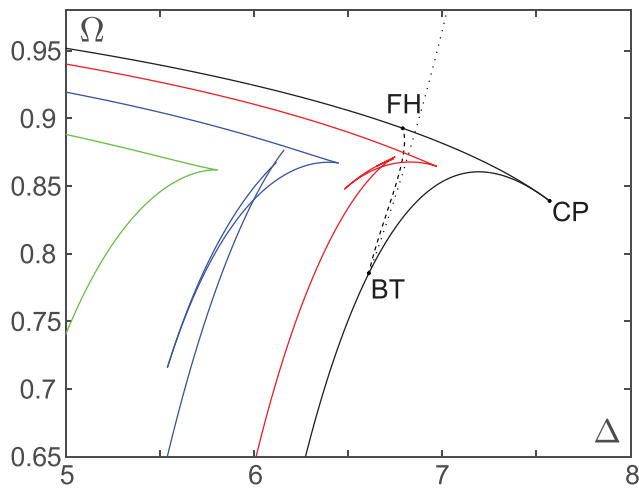


FIG. 5. The saddle-node bifurcation curves on the (Δ, Ω) -plane are plotted for several values of the noise strength: from right to left, $\sigma = 0$ (black), $\sigma = 0.3$ (red), $\sigma = 0.5$ (blue), and $\sigma = 0.7$ (green). The system has three (or more) equilibrium states inside the tongue-shaped domain and a single state outside. The black dashed line and the black dotted line show the saddle homoclinic and Hopf bifurcations in the noiseless case, respectively. The cusp (CP), Bogdanov-Takens (BT), and fold-homoclinic (FH) points are also shown for the noiseless case.

large ensemble of size N , the noise creates fluctuations in the mean field $\propto \sigma/\sqrt{N}$. For $N \rightarrow \infty$, these fluctuations disappear and one can observe the coexistence of locally stable regimes of macroscopic dynamics, while for finite N , fluctuations are present and lead to spontaneous switchings between the regimes.^{31,32} For regimes that are close to each other in the phase space, the switching becomes very frequent, which makes the observation of separate regimes practically impossible.

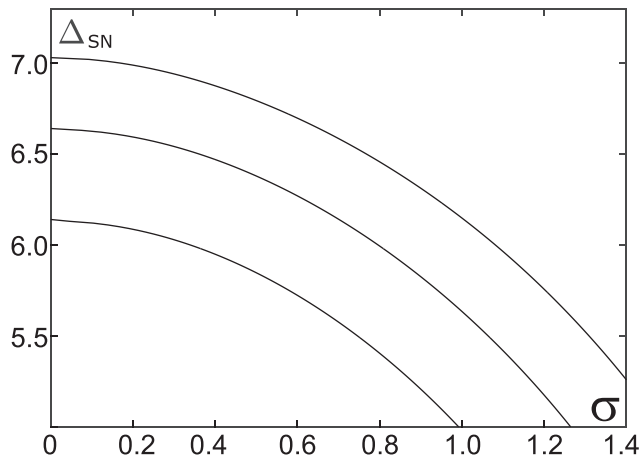


FIG. 6. Bifurcation threshold Δ_{SN} is plotted vs the noise strength σ for several values of Ω : from top to bottom, $\Omega = 0.88$, $\Omega = 0.90$, and $\Omega = 0.92$.

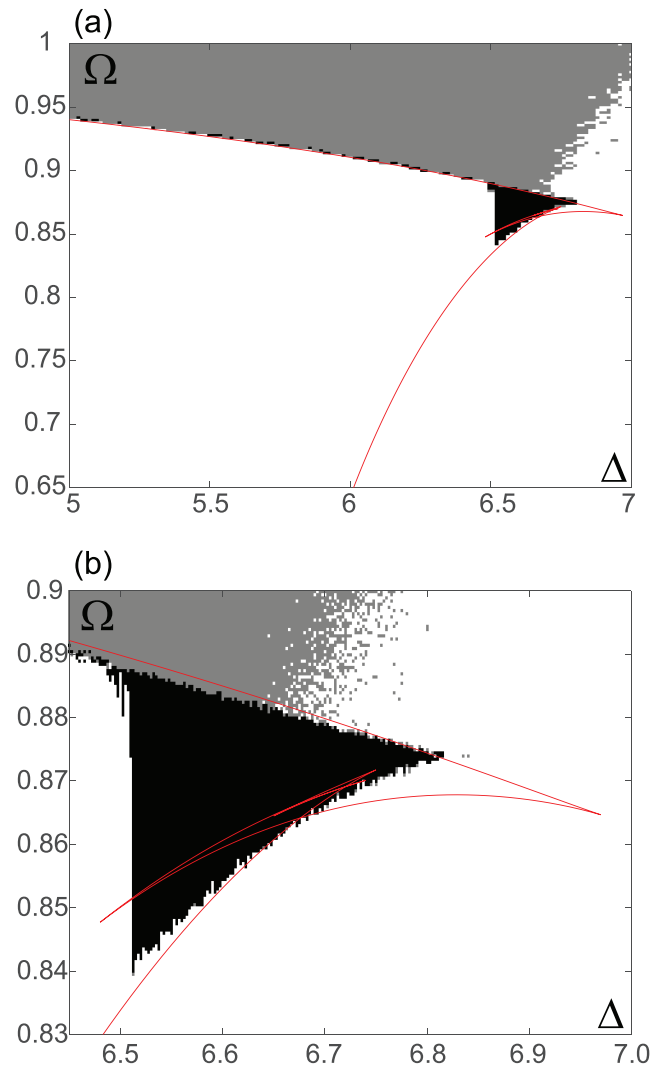


FIG. 7. (a) The domains of bistability (black) and collective oscillations (gray) for a finite ensemble of $N = 10^4$ elements on the (Δ, Ω) -plane are plotted for $\sigma = 0.3$. Red lines show the theoretically obtained saddle-node bifurcation curves (the same as in Fig. 5). (b) Zoom-in of the bistability domain from graph (a).

VI. CONCLUSION

In this paper, the method of circular cumulants has been applied to describe the collective dynamics of a heterogeneous ensemble of globally coupled active rotators subject to intrinsic noise. The method has allowed us to obtain a reduced model describing the dynamics of “local” subpopulations of elements with a specific frequency. It was shown that with the reduced model, one can calculate the values of the local order parameters with a decent accuracy: for a weak noise, in most cases, the method error is of the order of magnitude of σ^4 . The accuracy drops significantly close to

the critical frequency values, where the local dynamics of the elements experiences a SNIPER bifurcation. In this case, the method error is of the order of magnitude of $\sigma^{2/3}$. However, the width of the frequency range, where the cumulant method gives a significant error, becomes narrower as the noise strength decreases according to the power law $\sigma^{4/3}$. As a result, the error in the calculation of the global order parameter is of the order of magnitude of σ^2 . This level of accuracy turns out to be acceptable for using the two-cumulant model reduction as an approximation for the two following reasons. First, in some systems,²¹ even a small noise can create stable regimes far from the Ott–Antonsen manifold; in these systems, the effect of noise is large compared to σ^2 . Second, the error of solutions turns out to be small compared to the noise-induced effects, although the solutions do not become more relatively accurate for $\sigma \rightarrow 0$.

The obtained expressions for the order parameter of “local” subpopulations have been used to derive the self-consistency condition for stationary collective modes of the population behavior, characterized by a constant-in-time Kuramoto order parameter (mean field). For a uniform distribution of natural frequencies in a population, the self-consistency condition reduces to a scalar equation for the order parameter. The solutions of this equation allow one to determine the stationary regimes of the system and to reconstruct its microscopic state. Depending on the parameters, the system can have either one or several solutions. The latter case corresponds to the bistability in the system, which can demonstrate different locally stable modes of collective behavior for the same parameter values. The bistability domain in the parameter space has a characteristic tongue-like shape; the theory developed in this paper allows one to find the boundaries of this domain fairly accurately. It also allows us to determine the border between the stationary and oscillatory collective modes. The study explicitly reveals that the impact of intrinsic noise is qualitatively equivalent to an increase of the population heterogeneity quantified by the width of the distribution of element parameters.

ACKNOWLEDGMENTS

The work of V.V.K. and D.A.Z. on the analysis of the heterogeneous population was supported by the Russian Foundation for Basic Research (Project No. 20-52-1202). The work of V.V.K. and D.A.Z. on numerical simulations was supported by the Russian Science Foundation (Project No. 19-72-10114). The work of B.S.M. and D.S.G. on general issues of the construction of cumulant expansions in the presence of singularities was supported by the Russian Science Foundation (Project No. 19-42-04120).

DATA AVAILABILITY

The data that support the findings of this study are available within the article.

REFERENCES

- ¹A. Pikovsky, M. Rosenblum, and J. Kurths, *Synchronization: A Universal Concept in Nonlinear Sciences* (Cambridge University Press, Cambridge, 2003).
- ²B. Ermentrout, “Neural networks as spatio-temporal pattern-forming systems,” *Rep. Prog. Phys.* **61**, 353–430 (1998).
- ³R. E. Mirollo and S. H. Strogatz, “Synchronization of pulse-coupled biological oscillators,” *SIAM J. Appl. Math.* **50**, 1645–1662 (1990).

- ⁴K. P. O’Keefe and S. H. Strogatz, “Dynamics of a population of oscillatory and excitable elements,” *Phys. Rev. E* **93**, 62203 (2016).
- ⁵Y. Kuramoto, “International symposium on mathematical problems in theoretical physics,” *Lecture Notes Phys.* **30**, 420 (1975).
- ⁶J. D. Crawford, “Amplitude expansions for instabilities in populations of globally-coupled oscillators,” *J. Stat. Phys.* **74**, 1047–1084 (1994).
- ⁷J. A. Acebrón, L. L. Bonilla, C. J. P. Vicente, F. Ritort, and R. Spigler, “The Kuramoto model: A simple paradigm for synchronization phenomena,” *Rev. Mod. Phys.* **77**, 137–185 (2005).
- ⁸V. Klinshov and I. Franović, “Two scenarios for the onset and suppression of collective oscillations in heterogeneous populations of active rotators,” *Phys. Rev. E* **100**, 62211 (2019).
- ⁹S. Shinomoto and Y. Kuramoto, “Phase transitions in active rotator systems,” *Prog. Theor. Phys.* **75**, 1105 (1986).
- ¹⁰H. Sakaguchi, S. Shinomoto, and Y. Kuramoto, “Mutual entrainment in oscillator lattices with nonvariational type interaction,” *Prog. Theor. Phys.* **79**, 1069 (1988).
- ¹¹A. V. Dolmatova, D. S. Goldobin, and A. Pikovsky, “Synchronization of coupled active rotators by common noise,” *Phys. Rev. E* **96**, 062204 (2017).
- ¹²H. Sakaguchi, S. Shinomoto, and Y. Kuramoto, “Phase transitions and their bifurcation analysis in a large population of active rotators with mean-field coupling,” *Prog. Theor. Phys.* **79**, 600–607 (1988).
- ¹³S. H. Park and S. Kim, “Noise-induced phase transitions in globally coupled active rotators,” *Phys. Rev. E* **53**, 3425 (1996).
- ¹⁴M. A. Zaks, A. B. Neiman, S. Feistel, and L. Schimansky-Geier, “Noise-controlled oscillations and their bifurcations in coupled phase oscillators,” *Phys. Rev. E* **68**, 66206 (2003).
- ¹⁵C. J. Tessone, A. Scire, R. Toral, and P. Colet, “Theory of collective firing induced by noise or diversity in excitable media,” *Phys. Rev. E* **75**, 16203 (2007).
- ¹⁶J. A. Acebrón and L. L. Bonilla, “Asymptotic description of transients and synchronized states of globally coupled oscillators,” *Physica D* **114**, 296–314 (1998).
- ¹⁷I. V. Tyulkina, D. S. Goldobin, L. S. Klimenko, and A. Pikovsky, “Dynamics of noisy oscillator populations beyond the Ott–Antonsen ansatz,” *Phys. Rev. Lett.* **120**, 264101 (2018).
- ¹⁸D. S. Goldobin, I. V. Tyulkina, L. S. Klimenko, and A. Pikovsky, “Collective mode reductions for populations of coupled noisy oscillators,” *Chaos* **28**, 101101 (2018).
- ¹⁹I. V. Tyulkina, D. S. Goldobin, L. S. Klimenko, and A. S. Pikovsky, “Two-bunch solutions for the dynamics of Ott–Antonsen phase ensembles,” *Radiophys. Quantum Electron.* **61**, 640–649 (2019).
- ²⁰D. S. Goldobin and A. V. Dolmatova, “Ott–Antonsen ansatz truncation of a circular cumulant series,” *Phys. Rev. Res.* **1**, 33139 (2019).
- ²¹D. S. Goldobin and A. V. Dolmatova, “Circular cumulant reductions for macroscopic dynamics of Kuramoto ensemble with multiplicative intrinsic noise,” *J. Phys. A: Math. Theor.* **53**, 08LT01 (2020).
- ²²A. Campa, “Phase diagram of noisy systems of coupled oscillators with a bimodal frequency distribution,” *J. Phys. A: Math. Theor.* **53**, 154001 (2020).
- ²³A. T. Winfree, “Biological rhythms and the behavior of populations of coupled oscillators,” *J. Theor. Biol.* **16**, 15–42 (1967).
- ²⁴A. T. Winfree, *The Geometry of Biological Time* (Springer, 2001).
- ²⁵D. Pazó, “Thermodynamic limit of the first-order phase transition in the Kuramoto model,” *Phys. Rev. E* **72**, 46211 (2005).
- ²⁶E. Ott and T. M. Antonsen, “Low dimensional behavior of large systems of globally coupled oscillators,” *Chaos* **18**, 37113 (2008).
- ²⁷E. Ott and T. M. Antonsen, “Long time evolution of phase oscillator systems,” *Chaos* **19**, 23117 (2009).
- ²⁸E. Lukacs, *Characteristic Functions* (Griffin, London, 1970).
- ²⁹A. N. Malahov, *Cumulant Analysis of Random Non-Gaussian Processes and Their Transformations [in Russian]* (Soviet Radio, Moscow, 1978).
- ³⁰J. Marcinkiewicz, “Sur une propriété de la loi de Gauss,” *Math. Z.* **44**, 612–618 (1939).
- ³¹I. Franović and V. Klinshov, “Slow rate fluctuations in a network of noisy neurons with coupling delay,” *Europhys. Lett.* **116**, 48002 (2016).
- ³²I. Franović and V. Klinshov, “Clustering promotes switching dynamics in networks of noisy neurons,” *Chaos* **28**, 023111 (2018).